

## Article

# Spin Transition Kinetics in the Salt [H<sub>2</sub>N(CH<sub>3</sub>)<sub>2</sub>]<sub>6</sub>[Fe<sub>3</sub>(L)<sub>6</sub>(H<sub>2</sub>O)<sub>6</sub>] (L = 4-(1,2,4-triazol-4-yl)ethanedisulfonate)

Cristina Sáenz de Pipaón <sup>1</sup>, Pilar Maldonado-Illescas <sup>1</sup>, Verónica Gómez <sup>2</sup> and José Ramón Galán-Mascarós <sup>1,3,\*</sup>

- <sup>1</sup> Institute of Chemical Research of Catalonia (ICIQ), The Barcelona Institute of Science and Technology, Avinguda Països Catalans 16, Tarragona E-43007, Spain; csaenzpipaon@iciq.es (C.S.P.); pmaldonado@iciq.es (P.M.-I.)
- <sup>2</sup> Institute of Nanotechnology, Karlsruhe Institute of Technology (KIT), Hermann-von-Helmholtz-Platz 1, Eggenstein-Leopoldshafen 76344, Germany; veronica.piedrafita@kit.edu
- <sup>3</sup> Catalan Institution for Research and Advanced Studies (ICREA), Passeig Lluís Companys 23, Barcelona E-08010, Spain
- \* Correspondence: jrgalan@iciq.es; Tel.: +34-977-920-808

Academic Editors: Guillem Aromí, José Antonio Real and Carlos J. Gómez García

Received: 15 January 2016; Accepted: 7 March 2016; Published: 28 March 2016

**Abstract:** The dimethylammonium salt of the Fe<sup>II</sup> polyanionic trimer [Fe<sub>3</sub>(μ-L)<sub>6</sub>(H<sub>2</sub>O)<sub>6</sub>]<sup>6−</sup> (L = 4-(1,2,4-triazol-4-yl)ethanedisulfonate) exhibits a thermally induced spin transition above room temperature with one of the widest hysteresis cycles observed in a spin crossover compound (>85 K). Furthermore, the metastable high-spin (HS) state can be thermally trapped via relatively slow cooling, remaining metastable near room temperature, with a characteristic  $T_{\text{TIESST}} = 250$  K (TIESST = temperature-induced excited spin-state trapping). The origin for this unique behavior is still uncertain. In this manuscript, we report detailed studies on the relaxation kinetics of this system in order to disclose the mechanism and cooperativity controlling this process.

**Keywords:** spin crossover; hysteresis; relaxation kinetics; iron; triazole

## 1. Introduction

Spin crossover (SCO) complexes are some of the most fascinating bistable materials in molecular magnetism [1–3]. In such metal complexes, a high spin (HS) excited state can be populated by external stimuli from the ground low spin (LS) state: thermally, under light irradiation, under pressure, *etc.* In the solid state, this spin transition may be associated to a crystallographic transition, due to the chemical and volumetric differences between LS and HS configurations [4]. This synergy gives rise to cooperative spin transitions where the metastable HS state is entropically favored. Such cooperative transitions may also show thermal hysteresis. SCO materials exhibiting bistability at and above room temperature are well-known [5] and technologically relevant. On the contrary, most other molecule-based magnetic materials exhibit their unique striking properties only at very low temperatures, close to liquid He, precluding their wide application. Because of all of these reasons, SCO materials have been postulated as future components for devices such as stimuli-responsive molecular switches for multifunctional materials, memories, electrical circuits, or displays [5,6].

Fe(II) complexes represent the most numerous and remarkable family of SCO materials, matching all these requirements [7,8]. Several materials exhibit room temperature switchability [9] and ultra-fast light controlled responses [10–14]. In addition to their intrinsic properties, these SCO materials can be also used as probes to switch a second property in a hybrid multicomponent system [15,16].

In our group, we have developed a new family of SCO materials based on the trinuclear  $\text{Fe}^{\text{II}}$  polyanion  $[\text{Fe}_3(\mu\text{-L})_6(\text{H}_2\text{O})_6]^{6-}$  ( $\text{L} = 4\text{-(1,2,4-triazol-4-yl)ethanedisulfonate}$ ) [17]. This is the first polyanionic species exhibiting SCO phenomena. As its dimethylammonium salt, a wide hysteresis cycle (over 90 K) was observed just above room temperature. More remarkably, easy excited HS-HS-HS state thermal trapping and unparalleled slow kinetics were found in the cooling branches of the hysteresis cycles. The temperature of temperature-induced excited spin-state trapping (TIESST) for this compound is a record high, the highest ever observed up to now for any thermally trapped excited state in a switchable material, including SCO and charge transfer compounds [18–20]. Typically, cooperative/abrupt transitions are associated with wide hysteresis. The hysteresis cycle can be scan-rate-dependent in such systems for crystallographically constrained complexes [21], but the spin transition itself remains abrupt in all experiments.

The cooperativity between SCO centers plays a key role in the abruptness of the transition and the appearance of thermal hysteresis. Low cooperativity implies a gradual spin transition (tens of Kelvin), similar to the one observed in isolated SCO centers, such as in solution. Thus, hysteresis is theoretically not possible, since the population of the excited state will depend exclusively on the temperature from the Boltzmann distribution. In highly cooperative systems, the transition is abrupt (usually less than 10 K) and hysteresis can appear because the SCO is associated with a crystallographic transition. For the reported compound, the transition is gradual and occurs along several tens of Kelvin, which suggests a low cooperative system. However, a wide hysteresis is observed. This is counterintuitive, since significant interactions between SCO centers are expected in such case. Here, we present detailed kinetic studies on the relaxation process of this SCO material in the search for the origin of such wide hysteresis process in a material with apparently non-cooperative behavior.

## 2. Results and Discussion

The crystalline structure of the ammonium salt  $(\text{Me}_2\text{NH}_2)_6[\text{Fe}_3(\mu\text{-L})_6(\text{H}_2\text{O})_6]$  (1) at 100 K contains a linear array of octahedral  $\text{Fe}^{\text{II}}$  ions [17]. The terminal metal centers are connected to the central one by a triple  $\mu\text{-triazole}$  bridge, and complete their coordination sphere with three water molecules (Figure 1a). The metal to ligand bonding distances indicates that the central  $\text{Fe}^{\text{II}}$  ion is in low spin state and the terminal ones in high spin. The Fe clusters are well isolated from each other by cations and solvent molecules. Intermolecular connectivity is defined by an extensive H-bond network involving the dangling sulfonate moieties from the ethane groups, the dimethylammonium cations, and water molecules, with short intermolecular O–O distances (2.6–2.9 Å).

Through X-ray diffraction analysis, we conclude that the room temperature crystal structure is isostructural to that solved at 100 K (Figure 1c). Furthermore, in Figure 1d, we show the evolution of the X-ray powder pattern when heating the sample up to 420 K. Crystallinity deteriorates fast upon heating, with all reflections disappearing above 410 K. When cooling, the sample crystallinity is not recovered, and the material remains amorphous upon successive cycles. This confirms that crystallographic phase transitions are not affecting the magnetic behavior of the system.

Magnetic measurements have showed the appearance of a thermal spin transition with a wide hysteresis above room temperature (Figure 2a). Such a wide hysteresis is typically associated with highly cooperative systems, where the crystallographic spin transition is responsible for the memory effect triggered by the SCO behavior. However, this material shows also very gradual spin transitions, with very slow kinetics compared to what should be associated with low cooperativity. Both observations are counterintuitive. In addition, the spin transition during the cooling branch, from HS-HS-HS to HS-LS-HS, can be easily quenched. The relaxation kinetics of this thermally trapped metastable HS-HS-HS state can clarify the degree of cooperativity in the crystal between SCO centers.

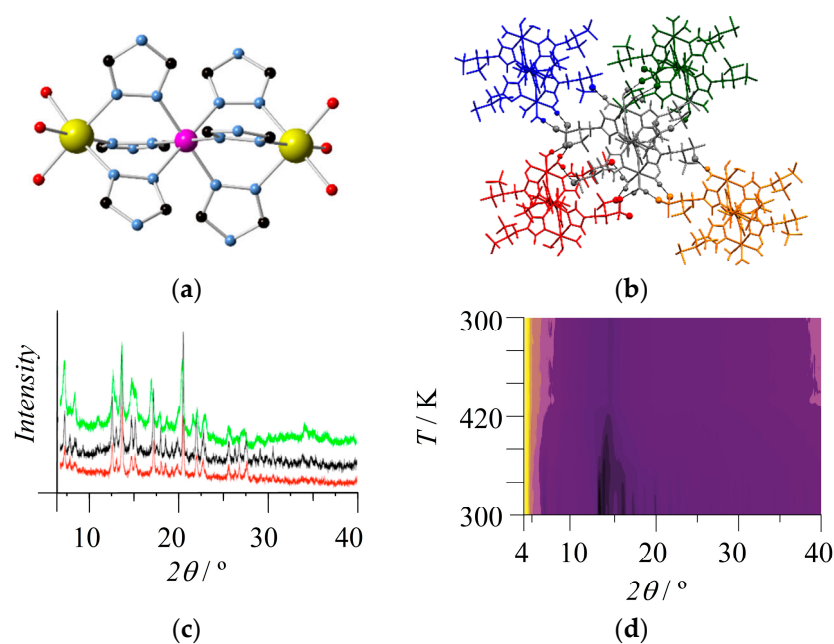


**Figure 1.** (a) Molecular structure of  $[\text{Fe}_3(\mu\text{-L})_6(\text{H}_2\text{O})_6]^{6-}$  (only the triazole group from the ligands is represented for clarity); (b) hydrogen bonding connectivity between multiple trimers in **1**; (c) X-ray diffraction powder pattern for **1** at room temperature as powder (green), single crystals (black), and after magnetic measurements in the 2–400 K; (d) temperature dependence of the X-ray diffraction powder pattern for **1** in the 300–420 K range at a scan rate of  $1 \text{ K min}^{-1}$ .

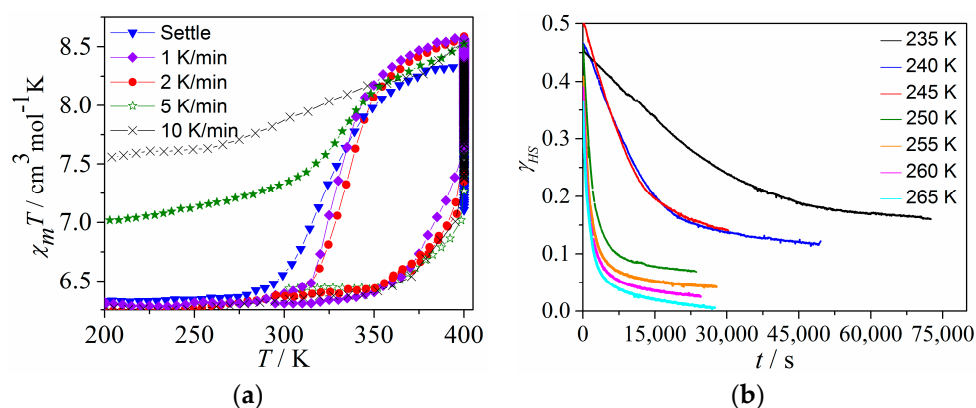


**Figure 2.** (a)  $\chi T$  vs.  $T$  plots for **1** at different heating/cooling rates; (b) relaxation of the trapped high spin (HS) HS-HS-HS fraction at different temperatures in the 265–235 K range; after cooling down, the sample at 10 K/min from saturation value at 400 K.

Multiple relaxation experiments were performed after heating a polycrystalline sample of **1** at 400 K for 6.5 h, and trapping the HS-HS-HS state, cooling it down to the desired temperature at a scan rate of 10 K/min. The time dependence of the magnetization at this point represents the kinetics of the relaxation process (Figure 2b). In order to normalize the data, we use as variable the fraction of HS-HS-HS complexes ( $\gamma_{\text{HS}}$ ) estimated from the equation:

$$\gamma_{\text{HS}}(t) = [(\chi T) - (\chi T)_{\text{LS}}] / [(\chi T)_{\text{HS}} - (\chi T)_{\text{LS}}], \quad (1)$$

where  $(\chi T)_{\text{LS}}$  is the magnetic value of the initial HS-LS-HS state, and  $(\chi T)_{\text{HS}}$  is the maximum magnetic value reached at 400 K for the corresponding sample batch.

The kinetics of a relaxation process can be described either with an exponential equation (single or stretched) [22] for non-cooperative systems, or with a sigmoidal curve for cooperative systems in a self-accelerating process [23]. The data obtained for 1 at all temperatures can be fitted, in a first order approximation, to an exponential process, which supports the low cooperativity of the system (Figure 3). This low cooperativity is in good agreement with the gradual transition observed in the thermal hysteresis cycle. This is also consistent with the weak intermolecular interactions between SCO complexes in the crystal.

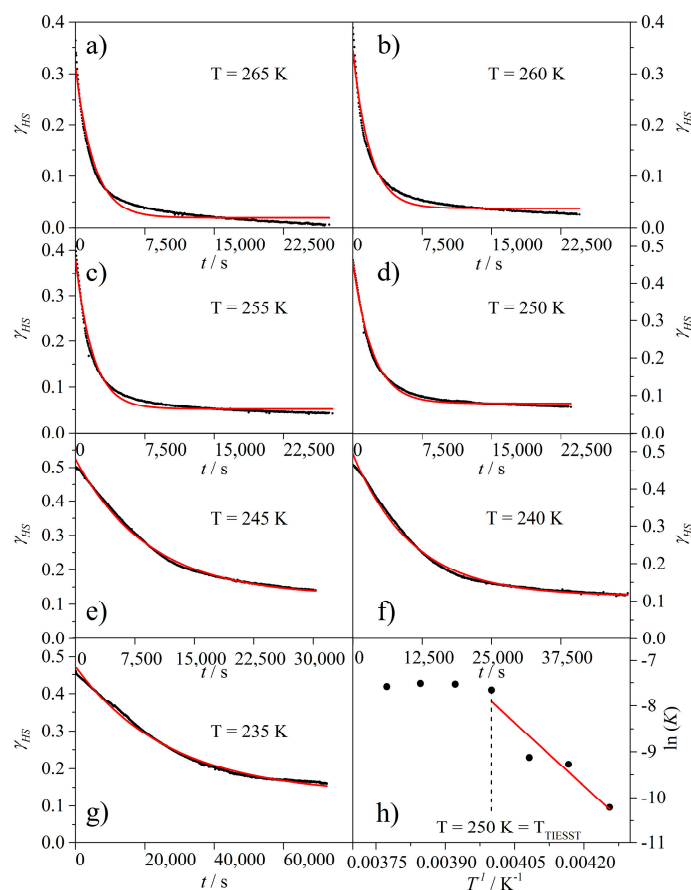


**Figure 3.** Fitting of the relaxation curves for the trapped HS-HS-HS fraction of 1 at different temperatures to exponential or sigmoidal expressions: (a) 265 K, (b) 260 K, (c) 255 K, (d) 250 K, (e) 245 K, (f) 240 K and (g) 235 K; (h) variation of  $k_{HL}$  as a function of  $T^{-1}$ .

Another remarkable observation in the relaxation kinetics deals with completion. In the temperature window we studied, total conversion to the HS-LS-HS ground state is not reached. Thus, at these temperatures, the population of both states reaches a kinetic equilibrium. Indeed, at low temperatures ( $<15$  K), the decrease in the  $\gamma_{HS}(t)$  is negligible and the relaxation curve remains flat in the timeframe of our experiments ( $<1\%$  decay after 4 h) [24]. To take this into account for the fitting model, we include this fraction  $\gamma_{\infty} = \gamma_{HS}(t \rightarrow \infty)$  in the exponential law, using the equation:

$$\gamma_{HS}(t) = \gamma_{\infty} + (\gamma_{HS} - \gamma_{\infty}) \exp(-k_{HL} \cdot t), \quad (2)$$

where  $k_{HL}$  depends on  $T$ , and can be expressed as:

$$k_{HL}(T) = k_{HL}^0 + k_{HL}^{\infty} \exp(E_a/k_B T) \quad (3)$$

where  $k_{HL}^0 = k_{HL}(T \rightarrow 0)$  and  $k_{HL}^{\infty} = k_{HL}(T \rightarrow \infty)$ .

An Arrhenius fit in the thermally activated region below the  $T_{\text{TIESST}}$  allows an estimation of the activation energy ( $E_a$ ) and the pre-exponential factor ( $k_{\text{HL}}^\infty$ ). Above  $T_{\text{TIESST}}$ , the relaxation process becomes temperature independent (Figure 3h). The term  $k_{\text{HL}}^0$  characterizes the relaxation in the quantum tunneling region, and it represents an upper limit at the lowest possible temperature [25]. In our case, due to the very high temperature range at which the experiments have been done, this parameter can be neglected. The energy barrier found with this model is  $E_a = 6370 \pm 1442 \text{ cm}^{-1}$  and  $k_{\text{HL}\infty} = 144 \times 10^{10} \text{ s}^{-1}$ . This represents the largest activation energy found in any SCO material, in good agreement with the  $T_{\text{TIESST}}$  (250 K). For example, in SCO compounds with  $T_{\text{TIESST}} = 99 \text{ K}$ , an activation energy of the  $934 \text{ cm}^{-1}$  was estimated [26].

The opposite transition from the HS-LS-HS to the HS-HS-HS state at high temperatures also shows slow kinetics, although much faster than in the previous case (Figure 4). An analogous treatment of the data in a thermally activated process was carried out using the equation:

$$\gamma_{\text{HS}}(t) = \gamma_\infty - (\gamma_\infty - \gamma_{\text{HS}}) \cdot \exp(-k_{\text{LH}} \cdot t), \quad (4)$$

where  $k_{\text{LH}}$  is analogous to  $k_{\text{HL}}$  (Equation (3)). The fitting is also better to an exponential expression, although not as satisfactory. This spin transition is much faster and does not show such a dependence on scan rate (Figure 2a). The poor fitting also suggests a more complex relaxation process, where several mechanisms could be at play.

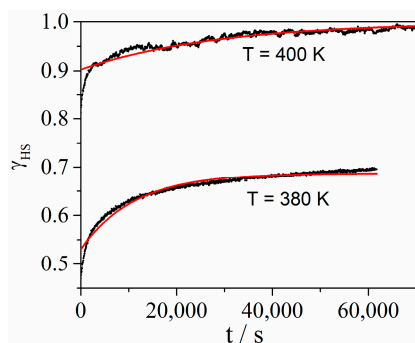


**Figure 4.** Fitting of the Low spin (HS-LS-HS) to High Spin (HS-HS-HS) transition for 1 at different temperatures to exponential expression.

In conclusion, compound 1 exhibits transition and relaxation kinetics typical of a non-cooperative system. This supports the molecular origin of the spin equilibrium, with a lesser contribution from the network. This is consistent with the exponential evolution of the metastable HS-HS-HS to HS-LS-HS relaxation (instead of sigmoidal). The much faster kinetics of the HS-LS-HS to HS-HS-HS transition point also in the same direction. We have associated the huge activation energy observed in the low temperature metastable HS-HS-HS state relaxation to the intramolecular electrostatic repulsion. The twelve dangling  $[\text{SO}_3]^-$  groups on the periphery of the ligands need to approach each other during this process, due to the shrinking of the  $\text{Fe}^{\text{II}}\text{--N}$  bonding distances (typically from  $>2.10 \text{ \AA}$  in HS to  $<1.95 \text{ \AA}$  in LS). On the contrary, the opposite transition requires expansion of the molecule, and electrostatic intramolecular repulsions should not play a major role. This would account for the remarkably different kinetics of both transitions, whereas purely crystallographic considerations would be of the same order in both processes. Although we still did not find direct proof of the molecular origin of the spin transition in this system, it is clear that the behavior is unique, and distinct to the well-known SCO materials with wide hysteresis and high transition temperatures, where abrupt transitions are observed. For the moment, the most plausible explanation is to assign the difference to a molecular origin, since crystallographically there are no additional magneto-structural correlations that can be claimed. Actually, this compound exhibits much weaker intermolecular interactions than most

other materials exhibiting SCO phenomena at such high temperatures [9]. For the sake of comparison, it is worth mentioning that an analogous (but neutral) trimer obtained with the monosulfonated triazole ligands does not show such slow kinetics, but typically abrupt transitions [27]. Diluted and solution experiments are underway in the search for additional experimental evidence to support our initial hypothesis.

### 3. Materials and Methods

All reagents were of commercial grade and used without further purification. Compound 1 was prepared following the literature procedure [17]. Magnetic measurements were carried out on polycrystalline powder samples with a Quantum Design MPMS-XL SQUID magnetometer (Quantum Design, Inc, San Diego, CA, USA) under a 1000-Oe field. Each sample was secured inside a gel capsule with glass wool, and the capsule was pinched (0.5-mm diameter hole) on the top to allow convenient purging of the interior of the capsule to allow for proper desolvation.

**Acknowledgments:** We acknowledge financial support from the European Union EU (ERC Stg grant 279313, CHEMCOMP), the Spanish Ministerio de Economía y Competitividad (MINECO) through the Severo Ochoa Excellence Accreditation 2014–2018 (SEV-2013-0319), the Generalitat de Catalunya (2014 SGR 797) and the Institute of Chemical Research of Catalonia ICIQ Foundation.

**Author Contributions:** J.R.G.-M. proposed the concept; J.R.G.-M. and C.S.P. conceived and designed the experiments; P.M.-I. and C.S.P. performed the experiments; C.S.P. analyzed the data; V.G. contributed reagents/materials/analysis tools; C.S.P. and J.R.G.-M. wrote the paper.

**Conflicts of Interest:** The authors declare no conflict of interest.

### References

1. Gütlich, P.; Goodwin, H.A., Eds.; *Spin Crossover in Transition Metal Compounds III*; Springer-Verlag: Berlin Heidelberg, Germany, 2004.
2. Bousseksou, A.; Molnar, G.; Salmon, L.; Nicolazzi, W. Molecular spin crossover phenomenon: Recent achievements and prospects. *Chem. Soc. Rev.* **2011**, *40*, 3313–3335. [[CrossRef](#)] [[PubMed](#)]
3. Muñoz, M.C.; Real, J.A. Thermo-, piezo-, photo- and chemo- switchable spin crossover iron(II)-metallocyanate based coordination polymers. *Coord. Chem. Rev.* **2011**, *255*, 2068–2093. [[CrossRef](#)]
4. Halcrow, M.A. Structure: Function relationships in molecular spin-crossover complexes. *Chem. Soc. Rev.* **2011**, *40*, 4119–4142. [[CrossRef](#)] [[PubMed](#)]
5. Kahn, O.; Martinez, C. Spin-transition polymers: From molecular materials toward memory devices. *Science* **1998**, *279*, 44–48. [[CrossRef](#)]
6. Letard, J.-F.; Guionneau, P.; Goux-Capes, L. Towards Spin Crossover Applications. In *Spin Crossover in Transition Metal Compounds III*; Springer-Verlag: Berlin Heidelberg, Germany, 2004; pp. 221–249.
7. Gütlich, P.; Gaspar, A.B.; Garcia, Y. Spin state switching in iron coordination compounds. *Beilstein J. Org. Chem.* **2013**, *9*, 342–391. [[CrossRef](#)] [[PubMed](#)]
8. Brooker, S. Spin crossover with thermal hysteresis: Practicalities and lessons learnt. *Chem. Soc. Rev.* **2015**, *44*, 2880–2892. [[CrossRef](#)] [[PubMed](#)]
9. Aromí, G.; Barrios, L.A.; Roubeau, O.; Gamez, P. Triazoles and tetrazoles: Prime ligands to generate remarkable coordination materials. *Coord. Chem. Rev.* **2011**, *255*, 485–546. [[CrossRef](#)]
10. Bertoni, R.; Cammarate, M.; Lorenc, M.; Matar, S.F.; Letard, J.-F.; Lemke, H.T.; Collet, E. Ultrafast light-induced spin-state trapping photophysics investigated in Fe(phen)<sub>2</sub>(NCS)<sub>2</sub> spin-crossover crystal. *Acc. Chem. Rev.* **2015**, *48*, 774–781. [[CrossRef](#)] [[PubMed](#)]
11. Sanchez-Costa, J.; Balde, C.; Carbonera, C.; Denux, D.; Wattiaux, A.; Desplanches, C.; Ader, J.-P.; Gütlich, P.; Letard, J.-F. Photomagnetic properties of an iron(II) low-spin complex with an unusually long-lived metastable LIESST state. *Inorg. Chem.* **2007**, *46*, 4114–4119. [[CrossRef](#)] [[PubMed](#)]
12. Guillaume, F.; Tobon, Y.A.; Bonhommeau, S.; Letard, J.-F.; Moulet, L.; Freysz, E. Photoswitching of the spin crossover polymeric material [Fe(Htrz)<sub>2</sub>(trz)](BF<sub>4</sub>) under continuous laser irradiation in a Raman scattering experiment. *Chem. Phys. Lett.* **2014**, *604*, 105–109. [[CrossRef](#)]



13. Craig, G.A.; Sanchez-Costa, J.; Roubeau, O.; Teat, S.J.; Shepherd, H.J.; Lopes, M.; Molnar, G.; Bousseksou, A.; Aromi, G. High-temperature photo-induced switching and pressure-induced transition in a cooperative molecular spin-crossover material. *Dalton Trans.* **2013**, *43*, 729–737. [[CrossRef](#)] [[PubMed](#)]
14. Murnaghan, K.D.; Carbonera, C.; Toupet, L.; Griffin, M.; Dirtu, M.M.; Desplanches, C.; Garcia, Y.; Collet, E.; Letard, J.-F.; Morgan, G.C. Spin-state ordering on one sub-lattice of a mononuclear iron(II) spin crossover complex exhibiting LIESST and TIESST. *Chem. Eur. J.* **2014**, *20*, 5613–5618. [[CrossRef](#)] [[PubMed](#)]
15. Koo, Y.S.; Galan-Mascaros, J.R. Spin crossover probes confer multistability to organic conducting polymers. *Adv. Mater.* **2014**, *26*, 6785–6789. [[CrossRef](#)] [[PubMed](#)]
16. Phan, H.; Benjamin, S.M.; Steve, E.; Brooks, J.S.; Shatruk, M. Photomagnetic response in highly conductive iron(II) spin-crossover complexes with TCNQ radicals. *Angew. Chem. Int. Ed.* **2015**, *54*, 823–827. [[CrossRef](#)] [[PubMed](#)]
17. Gómez, V.; Sáenz de Pipaón, C.; Maldonado-Illescas, P.; Waerenborgh, J.C.; Martin, E.; Benet-Buchholz, J.; Galán-Mascarós, J.R. Easy excited-state trapping and record high  $T_{\text{TIESST}}$  in a spin-crossover polyanionic  $\text{Fe}^{\text{II}}$  trimer. *J. Am. Chem. Soc.* **2015**, *137*, 11924–11927. [[CrossRef](#)] [[PubMed](#)]
18. Hauser, A.; Enachescu, C.; Daku, M.L.; Vargas, A.; Amstutz, N. Low-temperature lifetimes of metastable high-spin states in spin-crossover and in low-spin iron(II) compounds: The rule and exceptions to the rule. *Coord. Chem. Rev.* **2006**, *250*, 1642–1652. [[CrossRef](#)]
19. Wang, H.; Sinito, C.; Kaiba, A.; Costa, J.S.; Desplanches, C.; Dagault, P.; Guionneau, P.; Letard, J.-F.; Négrier, P.; Mondieig, D. Unusual solvent dependence of a molecule-based  $\text{Fe}^{\text{II}}$  macrocyclic spin-crossover complex. *Eur. J. Inorg. Chem.* **2014**, 4927–4933.
20. Li, D.; Clerac, R.; Roubeau, O.; Harte, E.; Mathoniere, C.; Le Bris, R.; Holmes, S.M. Magnetic and optical bistability driven by thermally and photoinduced intramolecular electron transfer in a molecular cobalt-iron prussian blue analogue. *J. Am. Chem. Soc.* **2008**, *130*, 252–258. [[CrossRef](#)] [[PubMed](#)]
21. Kulmaczewski, R.; Olguin, J.; Kitchen, J.A.; Feltham, H.L.C.; Jameson, G.N.L.; Tallon, J.L.; Brooker, S. Remarkable scan rate dependence for a highly constrained dinuclear iron(II) spin crossover complex with a wide thermal hysteresis loop. *J. Am. Chem. Soc.* **2014**, *136*, 878–881. [[CrossRef](#)] [[PubMed](#)]
22. Carbonera, C.; Dei, A.; Sangregorio, C.; Létard, J.-F. Optically switchable behaviour of a dioxolene adduct of a cobalt-macrocyclic complex. *Chem. Phys. Lett.* **2004**, *396*, 198–201. [[CrossRef](#)]
23. Hauser, A.; Jeftić, J.; Romstedt, H.; Hinek, R.; Spiering, H. Cooperative phenomena and light-induced bistability in iron(II) spin-crossover compounds. *Coord. Chem. Rev.* **1999**, *190–192*, 471–491. [[CrossRef](#)]
24. Paradis, N.; Chastanet, G.; Letard, J.-F. When stable and metastable HS states meet in spin-crossover compounds. *Eur. J. Inorg. Chem.* **2012**, *2012*, 3618–3624. [[CrossRef](#)]
25. Letard, J.-F. Photomagnetism of iron(II) spin crossover complexes—the  $T_{\text{LIESST}}$  approach. *J. Mater. Chem.* **2006**, *16*, 2550–2559. [[CrossRef](#)]
26. Paradis, N.; Chastanet, G.; Palamarciuc, T.; Rosa, P.; Varret, F.; Boukheddaden, K.; Letard, J.-F. Detailed investigation of the interplay between the thermal decay of the low temperature metastable HS state and the thermal hysteresis of spin-crossover solids. *J. Phys. Chem. C* **2015**, *119*, 20039–20050. [[CrossRef](#)]
27. Gómez, V.; Benet-Buchholz, J.; Martin, E.; Galán-Mascarós, J.R. Hysteretic spin crossover above room temperature and magnetic coupling in trinuclear transition-metal complexes with anionic 1,2,4-triazole ligands. *Chem. Eur. J.* **2014**, *20*, 5369–5379. [[CrossRef](#)] [[PubMed](#)]

